

Pulse-coupled resonate-and-fire models

Keiji Miura^{1,2,*} and Masato Okada^{2,3}

¹*Department of Physics, Graduate School of Sciences,
Kyoto University Kyoto 606-8502, Japan*

²*Laboratory for Mathematical Neuroscience,
RIKEN Brain Science Institute, Saitama 351-0198, Japan*

³*“Intelligent Cooperation and Control”, PRESTO, JST,
c/o RIKEN BSI, Saitama 351-0198, Japan*

Abstract

We analyze two pulse-coupled resonate-and-fire neurons. Numerical simulation reveals that an anti-phase state is an attractor of this model. We can analytically explain the stability of anti-phase states by means of a return map of firing times, which we propose in this paper. The resultant stability condition turns out to be quite simple. The phase diagram based on our theory shows that there are two types of anti-phase states. One of these cannot be seen in coupled integrate-and-fire models and is peculiar to resonate-and-fire models. The results of our theory coincide with those of numerical simulations.

PACS numbers: 87.19.La, 87.18.Sn, 05.45.Xt

*Electronic address: kmiura@brain.riken.jp

I. INTRODUCTION

The integrate-and-fire model [1] is well known in the context of spiking neuron models. However, it cannot reproduce voltage oscillations near the equilibrium state and resonance in response to sinusoidal current inputs seen in the Hodgkin-Huxley model [2, 3, 4]. Although we need a model with more than two variables to reproduce these phenomena [5], in general, it is difficult to solve models with more than two variables analytically.

Izhikevich suggested the resonate-and-fire model, which can reproduce voltage oscillations and resonance and is still analytically tractable [2]. The resonate-and-fire model is a 2-dimensional linear dynamical system with a threshold.

Voltage oscillations can play an important role in transmitting signals in the brain. For example, Izhikevich pointed out that resonance provided an effective tool in selective communication [2, 3, 4]. Therefore, we need to find out whether a network of resonate-and-fire models has properties that cannot be observed in integrate-and-fire models. The network properties of resonate-and-fire-like models (linearized FitzHugh-Nagumo models) have been investigated [6], but only an oscillatory regime where individual neurons fire spontaneously was considered and subthreshold voltage oscillations were not focused on.

In this paper, we analyze a system of two excitatory or inhibitory pulse-coupled resonate-and-fire models. We found that the system settled into an anti-phase state in both excitatory and inhibitory coupled cases in numerical simulations. We theoretically evaluated the stability of anti-phase states in detail. The system of pulse-coupled integrate-and-fire models has already been investigated [7], and it has been proved that for almost all initial conditions the system evolves to an in-phase state. This contrasts with resonate-and-fire models where the system does not necessarily evolve to an in-phase state.

In Sec. II, we briefly review the resonate-and-fire model and its properties. We then suggest a system for two pulse-coupled resonate-and-fire models.

In Sec. III, we demonstrate the existence of an anti-phase state and construct a theory that can be used to determine the region of existence for anti-phase states and assess their stability. We suggest an effective method of calculating the region. We show that global stability of anti-phase states can be determined by return maps and their local stability can be determined by a simple equation.

In Sec. IV, using the method proposed in Sec. III, we calculate a phase diagram for the

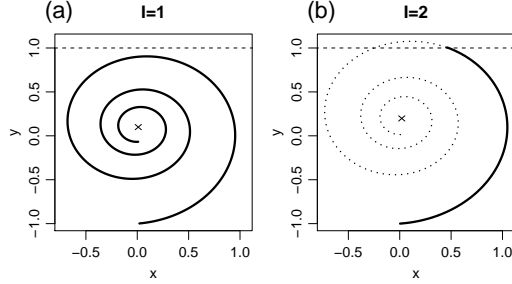


FIG. 1: Solutions for resonate-and-fire model. Orbits on xy plane are plotted. Cross represents fixed point. Dashed line is threshold. (a) Orbit for $I = 1$. Neuron does not fire. (b) Orbit for $I = 2$. Neuron fires. Neuron is immediately reset to $(x, y) = (0, -1)$ after it exceeds threshold. Dotted line is orbit neuron follows if not reset.

existence and local stability of anti-phase states. Stability switches near the boundary of the region of existence or at points where coupling strength is zero. We also determine stability by direct numerical simulations, and the results coincide with those of our theory. The phase diagram indicates there are two types of anti-phase states. The anti-phase state with a longer period is unique to coupled resonate-and-fire models and cannot be found in coupled integrate-and-fire models.

II. MODEL

A resonate-and-fire model is a 2-dimensional linear dynamical system with a threshold,

$$\begin{cases} \frac{dx}{dt} = -x - 10y + I \\ \frac{dy}{dt} = 10x - y, \end{cases} \quad (1)$$

where x and y are internal state variables and I is an external input. If y exceeds the threshold ($y = 1$), the internal state is reset to $(0, -1)$. Fig. 1 shows typical solutions. The neuron with $I = 1$ does not fire, while the neuron with $I = 2$ exceeds the threshold and fires. There is a critical value $I_C^1 = 1.56$, and neurons with $I > I_C^1$ can fire.

The resonate-and-fire model has a fixed point satisfying,

$$\begin{cases} 0 = \frac{dx}{dt} = -x - 10y + I \\ 0 = \frac{dy}{dt} = 10x - y. \end{cases} \quad (2)$$

The fixed point is $(x, y) = (\frac{I}{101}, \frac{10I}{101})$. When $I > I_C^2 = 10.1$, the fixed point is above the threshold and there is no stationary state. The eigenvalues of a linearized system at the

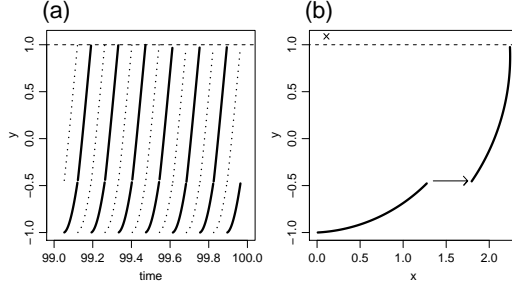


FIG. 2: Example of anti-phase states. $K = 0.5, I = 11$. (a) Time evolution of y . Horizontal axis represents time and vertical axis represents y . Solid lines and dotted lines represent each neuron. Dashed line is threshold ($y = 1$). Two neurons fire alternately at regular intervals. (b) Orbits in xy -plane. Arrow indicates jump in x -direction by pulse input and cross denotes fixed point, $(x, y) = (\frac{11}{101}, \frac{110}{101})$. Dashed line is threshold line. Here, both neurons follow same orbit, so two orbits overlap.

fixed point are $-1 \pm 10i$. Since the real part of the eigenvalue is negative, the fixed point is always stable if it exists. The imaginary part represents the angular velocity around the fixed point.

In this paper, we analyze a system of two pulse-coupled resonate-and-fire models,

$$\begin{cases} \frac{dx_i}{dt} = -x_i - 10y_i + I + K \sum \delta(t - t_k) \\ \frac{dy_i}{dt} = 10x_i - y_i, \end{cases} \quad (i = 1, 2) \quad (3)$$

where K is coupling strength. A neuron receives a pulse in the x -direction at the moment another neuron exceeds the threshold ($y = 1$). The neuron that has fired is immediately reset to $(x, y) = (0, -1)$. Our reset value is different from the original value, $(x, y) = (0, 1)$, in Izhikevich[2]. The reason is that with the original value, autocatalytic growth in the firing rate would accelerate indefinitely, leading to an explosion of the system. To avoid this, we chose a reset value that did not lie directly on the threshold. Since a neuron with our reset value has a refractory period, our reset value is suitable for a neuron model.

III. THEORY OF ANTI-PHASE STATES

A. Anti-phase states

We simulated the system of coupled resonate-and-fire models with $K = 0.5, I = 11$, and randomized initial conditions and found that it evolves to the state shown in Fig. 2(a). The solid lines and the dotted lines in the figure represent each neuron. The dashed line is the threshold ($y = 1$). The two neurons fire alternately at regular intervals. Since each neuron fires periodically, a phase can be defined with period 2π . We describe the firing time of one neuron as phase 0, which evolves in proportion to time. Here, the time at which another neuron fires is described by phase π . We call this state an anti-phase state. In general, we refer to a state where two neurons follow the same orbit but have phase shift π as an anti-phase state [8, 9, 10].

Fig. 2(b) plots the orbits in the x - y plane for the same data as in Fig. 2(a). The arrow indicates a jump in the x -direction by a pulse input and the cross denotes a fixed point, $(x, y) = (\frac{I}{101}, \frac{10I}{101})$. The dashed line is the threshold. Here, both neurons follow the same orbit, so the two orbits overlap in the figure. In the following, we theoretically examine in what parameter regions anti-phase states exist stably.

B. Existence of anti-phase states

Before we discuss the stability of anti-phase states, we derived a theory about the region of existence of anti-phase states.

We can obtain the solution orbits of anti-phase states analytically. Since the resonate-and-fire model is linear except for the moment of firing, we can integrate it piecewise. For ease of explanation, consider the imaginary plane and define

$$z \equiv x + iy. \tag{4}$$

Then, the resonate-and-fire model can be written as,

$$\frac{d}{dt}(z - z_*) = (-1 + 10i)z + I = (-1 + 10i)(z - z_*), \tag{5}$$

where,

$$z_* = \frac{I}{101} + \frac{10I}{101}i. \tag{6}$$

We can integrate it easily to,

$$z(t) = z_* + (z_0 - z_*)e^{(-1+10i)t}, \quad (7)$$

where z_0 denotes an initial condition at $t = 0$. For simplicity, let us consider an orbit that is reset at $t = 0$. The reset value is $(x, y) = (0, -1)$. Therefore, the initial condition is $z_0 = -i$ in the complex plane.

We assume the orbit receives a pulse input and jumps in the x -direction at $t = T$. Let $t = T$ in Eq. (7) and add K . Then, the neuronal state just after the pulse input becomes

$$z(T + 0) = z_* + (-i - z_*)e^{(-1+10i)T} + K. \quad (8)$$

Then, the orbit evolves to $t = T + T'$. The orbit at $t = T + T'$ is written using Eq. (8) as,

$$z(T + T') = z_* + (z(T + 0) - z_*)e^{(-1+10i)T'}. \quad (9)$$

The threshold line is $y = 1$ and the imaginary part of z is y . Thus, the condition for firing time is,

$$y(T + T') = \text{Im}(z(T + T')) = 1. \quad (10)$$

The orbit with $T' = T$ matches a situation where two neurons fire alternately at regular intervals. Thus, the condition that the orbit is an anti-phase state is,

$$y(2T) = 1. \quad (11)$$

Next, to set a limit to the T range satisfying $y(2T) = 1$ theoretically, we used the following theorem.

Theorem 1 *In anti-phase states, a neuron must fire within 360-degree rotation around the fixed point after a pulse input.*

Proof After 360-degree rotation, the orbit returns to the initial angle around the fixed point. However, the radius is smaller than the initial one. Then, the orbit that does not exceed the threshold within 360-degree rotation after a pulse input does not exceed forever. Thus, there is no anti-phase state where neurons do not fire within 360-degree rotation after a pulse input. ■

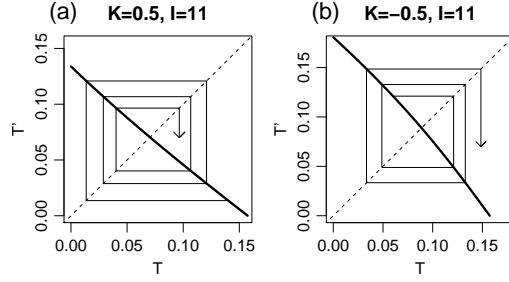


FIG. 3: (a) Bold line represents return map with $K = 0.5$ and $I = 11$. Dashed line is diagonal. Thin line with arrow is construction to obtain firing times. T approaches to fixed point by iteration of map. Anti-phase state is stable. (b) Return map with $K = -0.5$ and $I = 11$. T moves away from fixed point by iteration of map. Anti-phase state is unstable.

This theorem restricts the T range in which to search to a finite region. The restricted region is $0 < T < \frac{2\pi}{10}$ because the angular velocity around the fixed point is always 10 and it takes $\frac{2\pi}{10}$ to rotate by 360 degrees.

Thus, we should find a T value satisfying $y(2T) = 1$ in $0 < T < \frac{2\pi}{10}$, where the orbit must reach the threshold at time $2T$ for the first time after being reset. The condition that the orbit exceeds the threshold at time $2T$ for the first time after being reset can be mathematically represented as $y(t) < 1$ in $0 < t < 2T$.

C. Stability of anti-phase states

In this section, we derive a theory for the stability of anti-phase states.

T' satisfying $y(T+T') = 1$ (Eq. (10)) can be obtained as a function of T . Here T' denotes the interval between pulse input and firing and T denotes the interval between reset and pulse input. We refer to the map that maps T to T' as a return map. Fig. 3(a) plots the return map with $K = 0.5$ and $I = 11$.

In anti-phase states, the interval between pulse input and firing for one neuron equals the interval between reset and pulse input for another neuron. Thus, we can obtain the firing times of both neurons by using the return map iteratively. The thin line with the arrow in Fig. 3(a) demonstrates how to iterate the return map.

The intersection between the return map and diagonal line represents an anti-phase state and is a fixed point on the return map. For the return map in Fig. 3(a), the orbit finally

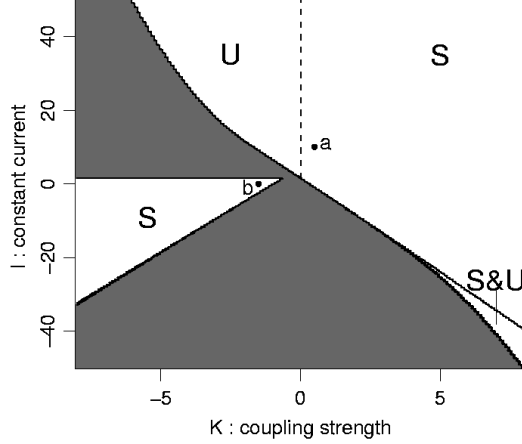


FIG. 4: Existence and stability of anti-phase states. In regions marked “S” or “U”, anti-phase state is stable or unstable. In region marked “S&U”, there are two types of anti-phase states. One of these is stable and the other is not. Dashed line is neutral stability ($K = 0$). There is no anti-phase state in dark region.

arrives at the fixed point starting from any initial value and the anti-phase state is globally stable. However, Fig. 3(b) demonstrates that the anti-phase state with $K = -0.5$ and $I = 11$ is unstable.

Although we can determine global stability by drawing return maps, we have to redraw them when we change the values of K and I . Therefore, it is difficult to monitor global stability over the whole range of K and I . In the following, we limit our focus to local stability and show that the condition of neutral stability is analytically obtained over the whole range of K and I . Local linear stability is determined as described below. We calculate the slope of the intersection between the return map and the diagonal line ($T' = T$). An anti-phase state is stable, if the absolute value of the slope is smaller than 1. Otherwise, it is unstable. When the slope is -1, an anti-phase state destabilizes through the period doubling bifurcation [11, 12, 13, 14]. When the slope is 1, a pair of anti-phase states disappears through saddle-node bifurcation.

We already derived the theory to determine the region of existence of anti-phase states in the previous section. Here, we will derive a condition for the neutral stability of anti-phase states.

We define $f(T, T')$ as a function of T and T' ,

$$f(T, T') \equiv y(T + T') = \text{Im}(z(T + T')), \quad (12)$$

where $y(T + T')$ is defined in Eq. (10). An anti-phase state is neutrally stable if the slope of its return map at the fixed point is -1, i.e.,

$$\frac{dT'}{dT} = -\frac{\left(\frac{df}{dT}\right)}{\left(\frac{df}{dT'}\right)} = -1, \quad (13)$$

where the derivative is evaluated at the fixed point. After additional calculations, the condition for neutral stability (Eq. (13)) becomes,

$$K(\tan(10T') - 10) = 0. \quad (14)$$

Note that Eq. (14) only depends on the sign of K and $T'(= T)$, and can be rewritten as,

$$K = 0, \quad (15)$$

$$T = \text{Arctan}(10)/10 = 0.1471128, \text{ and} \quad (16)$$

$$T = (\text{Arctan}(10) + \pi)/10 = 0.461272, \quad (17)$$

where capitalized Arctan denotes the principal value. An anti-phase state is neutrally stable, if any of the above three conditions are satisfied. Although arctan is a multivalued function, the theorem in the previous section restricts the T range to $0 < T < \frac{2\pi}{10}$ and we only need to consider two values of T .

We can rewrite the three conditions in terms of K and I by setting $T = T' = 0.1471128$ (or 0.461272) in Eq. (10). As a result, the three conditions for neutral stability become,

$$K = 0, \quad (18)$$

$$I = -5.056553K + 1.587449, \text{ and} \quad (19)$$

$$I = 4.58563K + 4.461462. \quad (20)$$

IV. RESULTS

We calculated the phase diagram for existence and stability of anti-phase states in the KI plane based on our theory. The results are plotted in Fig. 4. The anti-phase state is stable in the region marked ‘‘S’’ and unstable in that marked ‘‘U’’. In the region marked ‘‘S&U’’, there are two types of anti-phase states. One of these is stable and the other is not. The dashed line represents neutral stability (Eq. (18)). There are no anti-phase states in the dark region.

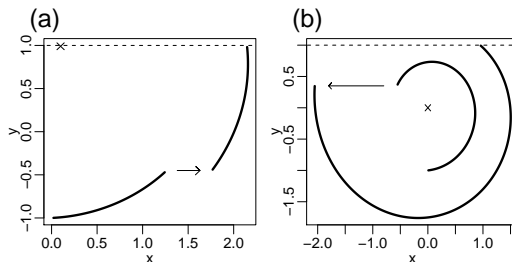


FIG. 5: Orbits of anti-phase states at points marked “a” and “b” in Fig. 4. Arrow indicates jump in x -direction by pulse input and cross denotes fixed point. Dashed line is threshold ($y = 1$). (a) Orbit with $K = 0.5$ and $I = 10$. (b) Orbit with $K = -1.5$ and $I = 0$.

To verify the theoretically obtained phase diagram in Fig. 4, we did numerical simulation using the Runge-Kutta method for numerous parameter values. We assessed an anti-phase state as stable if the orbit starting from it remained as it was. The results of numerical simulation coincided with those of our theory.

There are two distinct stable regions in Fig. 4. To determine the properties of these regions, we checked the orbits of anti-phase states at points marked “a” and “b” in Fig. 4. The results are in Fig. 5(a) and (b).

Fig. 5(a) plots the orbit of an anti-phase state with $K = 0.5$ and $I = 10$. The main characteristics of the orbit are that $K > 0$ and period T is relatively short. Since a pulse input just accelerates firing time, the orbit is not unique to coupled resonate-and-fire models and can also be seen in coupled integrate-and-fire models. The arrow indicates a jump in the x -direction by a pulse input and the cross denote the fixed point. The dashed line is the threshold ($y = 1$).

Fig. 5(b) plots the orbit of the anti-phase state with $K = -1.5$ and $I = 0$. The main characteristics of the orbit are that $K < 0$ and period T is relatively long. The orbit jumps in the negative direction by a pulse input and rebounds to fire as if it were a spring. This is unique to coupled resonate-and-fire models and cannot be seen in coupled integrate-and-fire models. In the region with $I > I_c^1 = 1.56$, there is no anti-phase state such as this, because a neuron spontaneously fires without pulse inputs there.

Fig. 6 is the magnification of Fig. 4 around $(K, I) = (0, 1.56)$. The figure illustrates that stability changes near the boundary of the region of existence and on line $K = 0$. In the region marked “S”, the anti-phase state is stable and unstable in “U”. The two dashed lines

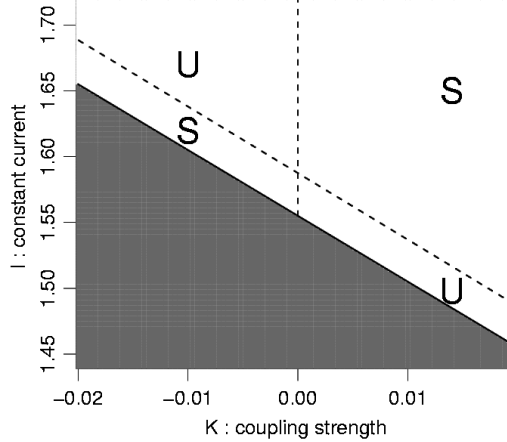


FIG. 6: Magnification of Fig. 4 around $(K, I) = (0, 1.56)$. In regions marked “S” or “U”, anti-phase state is theoretically stable or unstable. Two dashed lines represent neutral stability (Eq. (18) and Eq. (19)). There is no anti-phase state in dark region. Stability changes near boundary of region of existence and on line $K = 0$.

represent neutral stability (Eq. (18) and Eq. (19)). There is no anti-phase state in the dark region.

Two anti-phase states coexist in the region marked “S&U” in Fig. 4. To examine this region, we computed the period of anti-phase states at $K = 4$ as a function of I . The results are plotted in Fig. 7. The solid line denotes a stable state and the dashed line denotes an unstable one. At $I = -19.13$, two anti-phase states are created pairwise through the saddle-node bifurcation [11, 12, 13, 14]. In $-19.13 < I < -18.83$, the two states coexist. At $I = -18.83$, the unstable state disappears due to the effect of the threshold. In $I > -18.83$, only the stable state exists.

Fig. 8 plots the period of anti-phase states as a function of I at different values of K . The thick solid line denotes a stable state and the thick dashed line denotes an unstable one. The three thin lines are $m = -1, \infty$, and 1 . Here m is defined as the left hand side of Eq. (13), i.e., $m = \frac{dT'}{dT}$. At $m = 1$, two anti-phase states are created pairwise through the saddle-node bifurcation of the return map. At $m = -1$, the anti-phase state destabilizes through the period doubling bifurcation. Here, the condition that $m = -1$ becomes Eq. (16). At $m = \infty$, the anti-phase state disappears because the orbit is at a tangent to the threshold. In $K > K_c (= 1.31)$, two anti-phase states with different periods can coexist for some I ranges. One of these is stable and the other is not. In $K < K_c$, the anti-phase state destabilizes

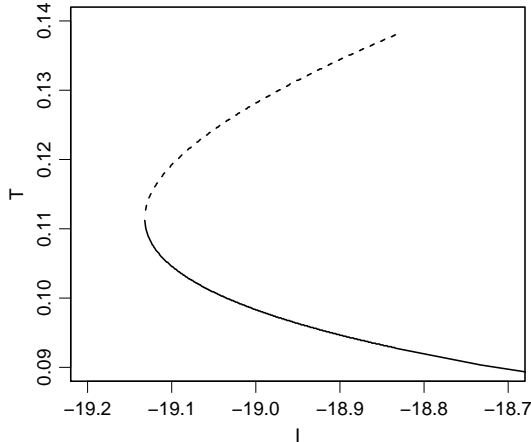


FIG. 7: Period of anti-phase states at $K = 4$ as function of I . Two states coexist in region. Solid line and dashed line denote stable state and unstable state, respectively. At $I = -19.13$, two anti-phase states are created pairwise through saddle-node bifurcation. In $-19.13 < I < -18.83$, two states coexist. At $I = -18.83$, unstable state disappears due to effect of threshold. In $I > -18.83$, only stable state exists.

crossing the line of $m = -1$. This is consistent with Fig. 6.

In $K < 0$ and $I < I_c^1 (= 1.56)$, there is also a region where two anti-phase states coexist and there is an unstable region near the boundary of the region of existence, as in $K > 0$. However, these regions are so small that we cannot see them in Fig. 4.

V. SUMMARY AND DISCUSSION

In this paper, we analyzed a system for two pulse-coupled resonate-and-fire models. We found that the system settled to an anti-phase state in numerical simulations. We looked for the existence and evaluated the stability of anti-phase states. We found an effective method of calculating the region of existence, where we set limits for the region theoretically and then utilized analytically obtained orbits. We found that stability of anti-phase states could be determined by means of a return map of firing times. The condition for neutral stability turned out to be unexpectedly simple (Eq. (14)). Based on our theory, we calculated a phase diagram for the existence and local stability of anti-phase states.

Stability changed near the boundary of the region of existence or at $K = 0$. We also determined stability by direct numerical simulations, and the results coincided with that

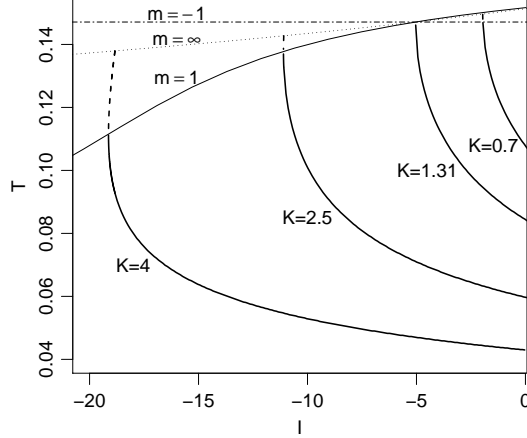


FIG. 8: Thick lines are periods of anti-phase states as functions of I at different values of K ($K = 0.7, 1.31, 2.5, 4$). Solid line and dashed line denote stable state and unstable state, respectively. Three thin lines are $m = -1, \infty$, and 1 , where m is defined as left hand side of Eq. (13), i.e., $m = \frac{dT'}{dT}$. At $m = 1$, two anti-phase states are created pairwise through saddle-node bifurcation of return map. At $m = -1$, anti-phase state destabilizes through period doubling bifurcation. Condition that $m = -1$ is Eq. (16). At $m = \infty$, anti-phase state disappears because orbit is tangential to threshold. In $K > K_c (= 1.31)$, two anti-phase states with different periods can coexist for some I ranges. One of these is stable and the other is not. In $K < K_c$, anti-phase state destabilizes crossing line of $m = -1$.

of our theory. The phase diagram revealed that there were two types of anti-phase states. An anti-phase state with a longer period is unique to coupled resonate-and-fire models and cannot be seen in coupled integrate-and-fire models.

We modeled a spike as a delta function. The case where a spike is modeled as an alpha function has been studied in [6]. However, stability condition was not obtained explicitly, and a phase diagram for existence of anti-phase states was not calculated as a function of coupling strength. Therefore, it is difficult to compare their results with ours.

In this paper, we focused on anti-phase states. What about in-phase states? If two neurons start under the same initial conditions, they must continue to follow the same orbit. Then, in-phase states exist at $I > I_C^1 (= 1.56)$ where a neuron can fire spontaneously. However, in-phase states are unstable against perturbations. This can be explained as follows. Let the orbits of two neurons differ infinitesimally. When the neurons fire in succession, the leading neuron receives a pulse input from the following neuron just after

being reset , while the following neuron receives a pulse input from the leading neuron just before firing. The positions where they receive pulse inputs differ considerably. The effects of pulse inputs on orbits are so different that the difference between orbits becomes finite. Thus in-phase states are always unstable.

Acknowledgments

We are grateful to S. Shinomoto and Y. Kuramoto for valuable discussions and suggestions of this work. This work was partially supported by Grant-in-Aid for Scientific Research on Priority Areas No. 14084212.

-
- [1] C. Koch, *Biophysics of computation* (Oxford Univ. Press, Oxford, 1999).
 - [2] E. M. Izhikevich, *Neural Networks* **14**, 883 (2001).
 - [3] E. M. Izhikevich, N. S. Desai, E. C. Walcott, and F. C. Hoppensteadt, *Trends. Neurosci.* **26**, 161 (2003).
 - [4] E. M. Izhikevich, *Biosystems* **67**, 95 (2002).
 - [5] E. M. Izhikevich, *Int. J. Bifurcat. Chaos.* **10**, 1171 (2000).
 - [6] A. D. Garbo, M. Barbi, and S. Chillei, *Int. J. Bifurcat. Chaos.* **11**, 2549 (2001).
 - [7] R. E. Mirollo and S. H. Strogatz, *Siam J. Appl. Math.* **50**, 1645 (1990).
 - [8] A. Pikovsky, M. Rosenblum, and J. Kurths, *Synchronization* (Cambridge Univ. Press, Cambridge, 2001).
 - [9] Y. Kuramoto, *Chemical oscillations, waves and turbulence* (Springer, Berlin, 1984).
 - [10] A. T. Winfree, *The geometry of biological time* (Springer, Berlin, 2001).
 - [11] J. Guckenheimer and P. Holmes, *Nonlinear oscillations, dynamical systems and bifurcations of vector fields* (Springer, Berlin, 1983).
 - [12] I. A. Kuznetsov and Y. A. Kuznetsov, *Elements of applied bifurcation theory* (Springer, Berlin, 1998).
 - [13] F. C. Hoppensteadt and E. M. Izhikevich, *Weakly connected neural networks* (Springer, Berlin, 1997).

- [14] S. Wiggins, *Introduction to applied nonlinear dynamical systems and chaos* (Springer, Berlin, 1990).